Pet Imaging of Bone Metastases Using Different Tracers

Einat Even-Sapir

Scintigraphy plays a major role in assessment of malignant bone involvement in cancer patients. Imaging is aimed to identify skeletal involvement as early as possible, to determine the extent of skeletal disease and to monitor response to therapy. Modern scintigraphic systems are integrated with CT. The combined functional-morphological fused data obtained is of clinical relevance for risk stratification detecting complications of bone metastases. Fused data may identify specific disease sites that require attention such as eminent fractures or tumor invasion to the spinal canal with risk for permanent neurologic deficits [1–4].

The concept of personalized medicine in treatment of cancer gave rise to the theranostics paradigm with the assumption that diagnostic test findings can accurately determine whether an individual is likely to benefit from a specific treatment. Nuclear medicine plays an essential role in theranostics by allowing SPECT or PET imaging of labeled molecular targets to assist in selecting patients with scintigraphy-positive disease sites for treatment with the same molecule labeled with high doses of β-emitting tracers [5].

The following chapter describes the role of PET/CT in assessment of malignant skeletal spread using four different PET tracers: ^{18}F-Fluordeoxyglucose (^{18}F-FDG), ^{68}Ga-Somatostatin and ^{68}Ga-Prostate Specific Membrane Antigen (PSMA). The forth tracer ^{18}F-Fluoride is a bone seeking agent high sensitive for detection of bone pathology either benign or malignant. The chapter also discusses the collaboration of PET imaging and treatment of bone metastases based on the teranostics paradigm.

^{18}F-FDG is the most commonly used PET tracer for imaging of various oncologic diseases. ^{68}Ga-Somatostatin is used in patients with neuroendocrine tumors and ^{68}Ga-PSMA PET has been recently introduced for imaging of patients with prostate cancer. All three PET tracers are characterized by direct accumulation by viable tumor cells. With this regard, the most prominent advantage of PET imaging with these tracers is that they accumulate in early marrow-based deposits (Figs. 1, 2 and 3). The vast majority of bone metastases initiate as bone marrow deposit of malignant cells. As the lesion enlarges, the surrounding bone undergoes osteoclastic (resorptive) and osteoblastic (depositional) activity and based on the balance between these two processes, lesions may appear radiographicaly as lytic, sclerotic (blastic) or mixed cortical lesions [1, 2, 6]. ^{99m}Tc-MDP bone scintigraphy (BS) and CT identify cortical metastases thus are insensitive for identification of early metastatic skeletal involvement when the tumor is confined to the marrow. The latter can be identified on PET using the tracers that accumulate in the tumor tissue regardless of the cortical accompanying changes [7].

Numerous publications have addressed the role of ^{18}F-FDG PET-CT in staging and follow up of cancer patients. ^{18}F-FDG PET imaging was shown to be superior to BS omitting the need to perform a separate BS for assessment of skeletal disease. In addition to its ability to detect metastasis confined to the marrow component, ^{18}F-FDG-PET is highly sensitive for detection of lytic type cortical metastases characterized by their high rate of glycolysis and hypoxia while BS is relatively insensitive for detection of this type of cortical lesions (Fig. 1a). Although ^{18}F-FDG-PET has been reported appropriate for detecting all types of bone metastases, it is considered to be somewhat less sensitive for detection of blastic type metastases that are considered generally less aggressive. Detection of the latter can be achieved, however, by reviewing the CT data of PET-CT [1–3, 6–8].

In spite of its proven relevance in various oncologic diseases, ^{18}F-FDG-PET/CT has no place in imaging patients with non-FDG avid tumors. Neuroendocrine tumors (NET) and prostate cancer are examples of basically non-FDG avid tumors for which we now have alternative suitable PET tracers. ^{68}Ga-Somatostatin PET-CT is of value for staging and follow-up of patients with the NET showing high-expression

E. Even-Sapir
Department of Nuclear Medicine, Tel Aviv Sourasky Medical Center, Sackler School of Medicine Tel Aviv University, 6 Weizman St, Tel Aviv, Israel
e-mail: evensap@tlvmc.gov.il

J. Hodler et al. (eds.), *Musculoskeletal Diseases 2017-2020*, DOI 10.1007/978-3-319-54018-4_27

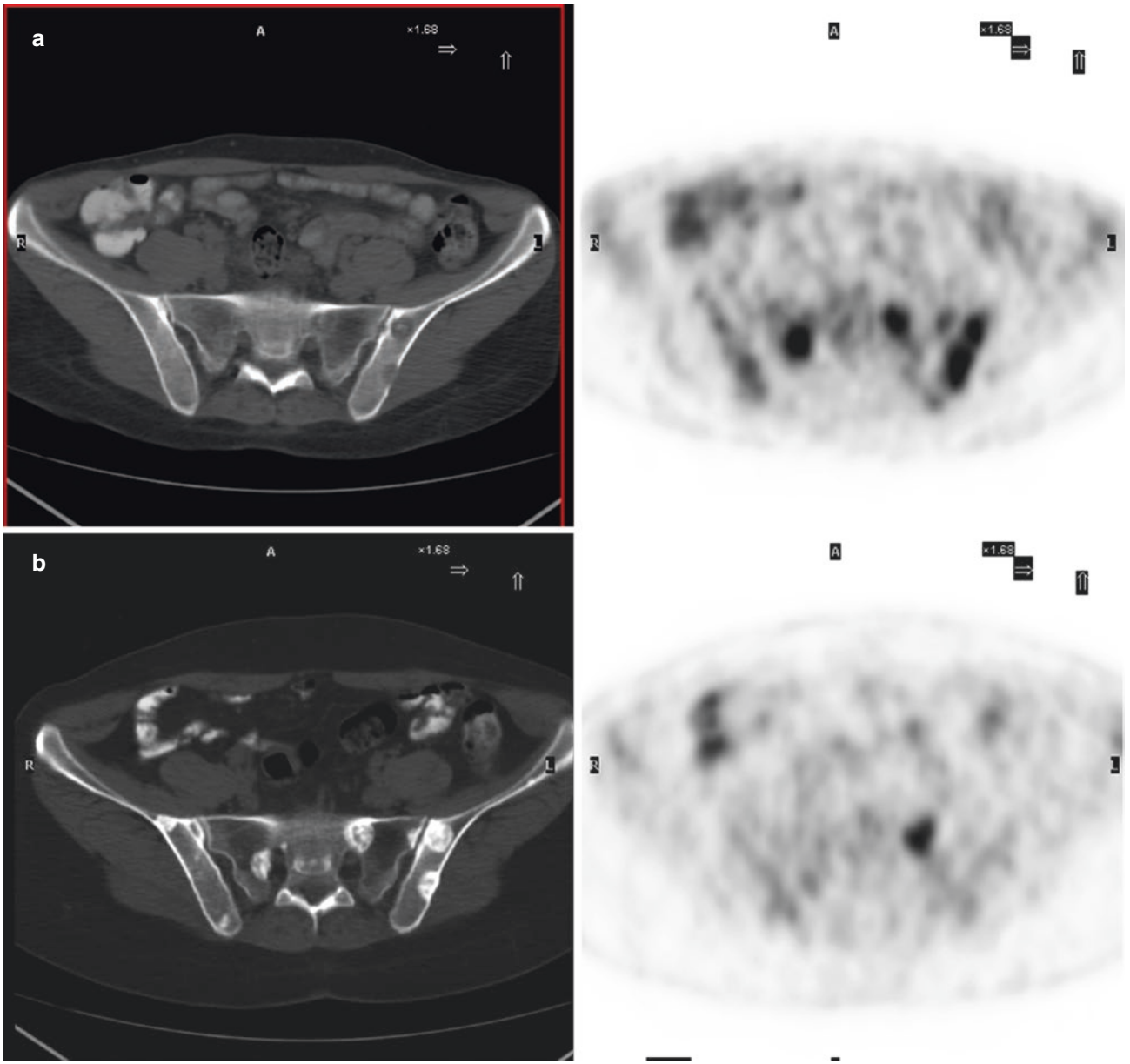

Fig. 1 ^{18}F-FDP identifying lytic and bone-marrow metastases at staging (**a**). After successful therapy the lesions appear sclerotic on CT with no increased uptake except for the lesion in the left sacrum which appears to be active with increased ^{18}F-FDG uptake in spite of the sclerotic changes that indicate repair (**b**)

of Somatostatin receptors. ^{68}Ga is a short lived PET tracer with a half-life of 68 min available from an in house generator of ^{68}Ge with a half-life of 270.8d independent of an onsite cyclotron. Analogues, mostly DOTA-derivatized peptides such as DOTA-Tyr3-octreotide (DOTATOC), show high affinity to Somatostatin receptors with beneficial pharmacokinetic properties. Combined with the better resolution of PET technology, ^{68}Ga-Somatostatin PET was reported to show high performance in assessment of bone involvement (Fig. 2a). It was found to be superior to BS, to CT and to gamma camera imaging with ^{111}In-Somatostatin (SRS). In a study on 89 patients with NET, SPECT STS identified only 72.5% and CT identified only 50% of the skeletal lesions identified by ^{68}Ga-Somatostatin PET [9–11].

PET with PSMA-ligands has gained attention as a promising imaging method in patients with prostate cancer. PSMA is a transmembrane protein with significantly elevated expression in most prostate cancer cells compared to benign prostatic tissue [12]. Comparison of ^{68}Ga-PSMA PET and planar BS for detection of skeletal involvement was the scope of a recently published manuscript. In a cohort of 126 patients with prostate cancer, sensitivity and specificity of PET were 98.7–100% and 88.2–100%, compared to 86.7–89.3% and 60.8–96.1% ($p < 0.001$) for BS, with ranges representing results for 'optimistic' or 'pessimistic' classification of equivocal lesions [13]. It should be noted, however that approximately 8% of prostate cancers do not show PSMA overexpression [14].

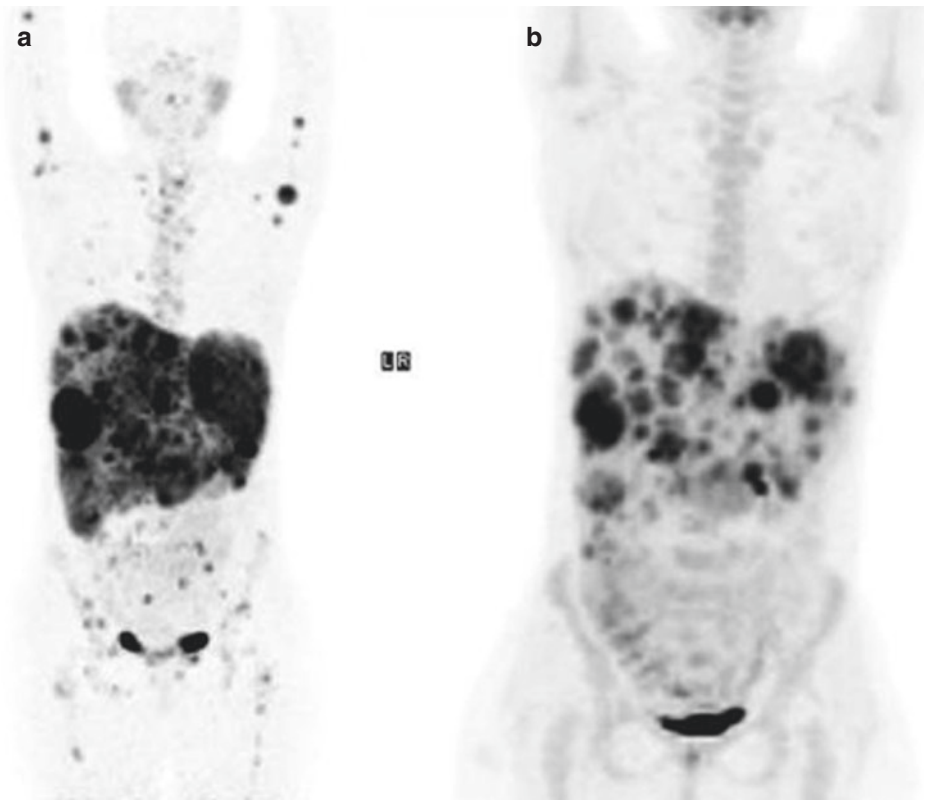

Fig. 2 Metastatic Carcinoid with extensive involvement of liver and bone marrow. ^{68}Ga-Somatostatin before (**a**) and after (**b**) PRRT therapy

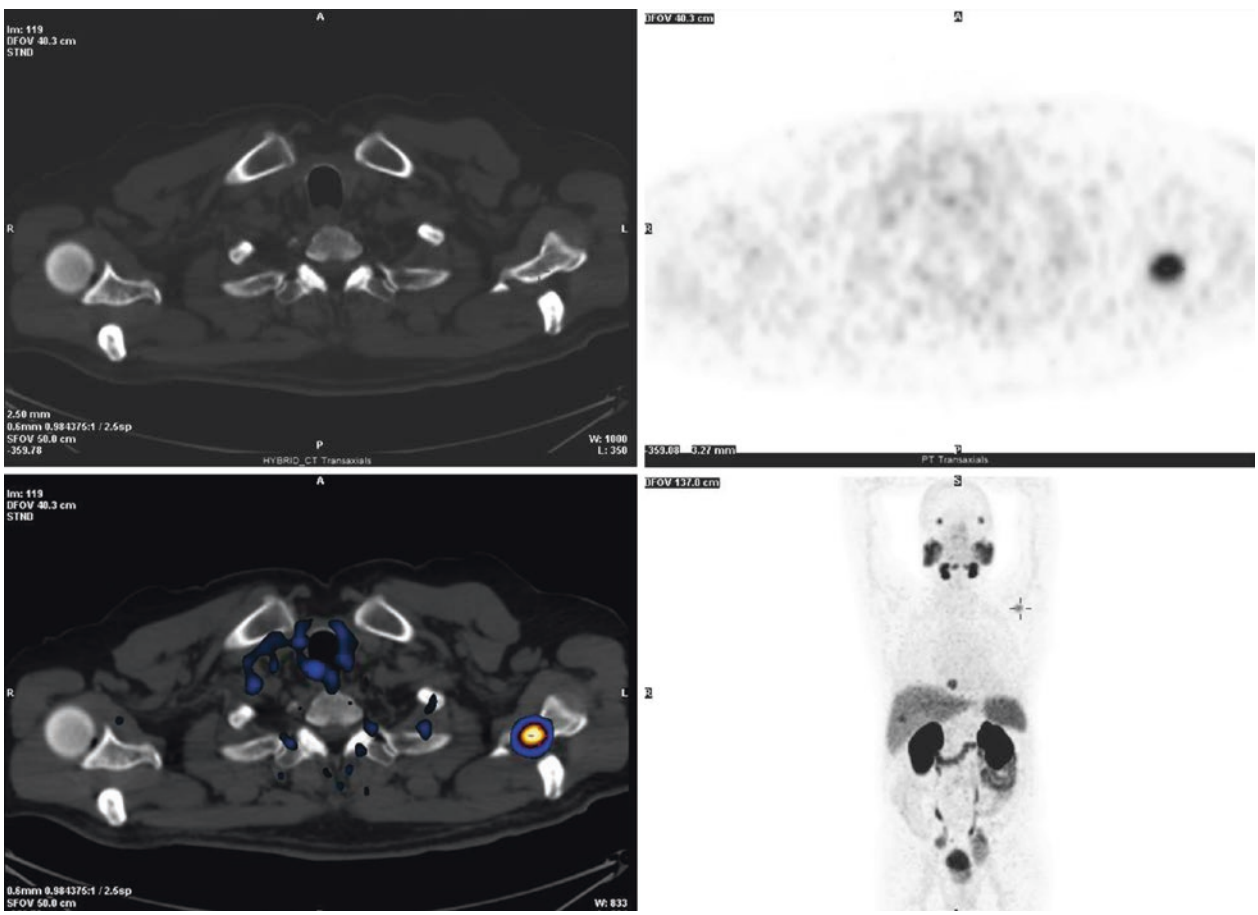

Fig. 3 ^{68}Ga-PSMA PET-CT in a patient with newly diagnosed high-risk prostate cancer identifying early marrow-based bone metastasis in the left scapula with morphological normal bone on CT

Monitoring response of bone metastases to therapy is an on going challenge on follow up imaging. Repair and active tumor may appear similar on BS and on CT, particularly when therapy protocol includes anti-osteoclastic agents such as bisphosphonates which encourage the appearance of sclerotic changes in the healing bone. The latter may remain permanent even when the metastasis is no longer active. ^{18}F-FDG, ^{68}Ga-Somatostatin and ^{68}Ga-PSMA accumulate only in active tumor tissue regardless of its morphologic appearance thus PET using these tracers can assist in separating repair of bone and active bone metastasis (Fig. 1b). Sequential ^{18}F-FDG PET-CT studies performed in patients with breast cancer have shown that ^{18}F-FDG uptake reflects the immediate tumor activity of bone metastases. Response is associated with decrease in intensity of uptake [15, 16]. Similarly, in NET, response of bone metastases after treatment can be evaluated efficiently by SRS or ^{68}Ga-Somatostatin PET (Fig. 2) [13, 14].

Same ligands of Somatostatin and of PSMA can be labeled with either ^{68}Ga for imaging purposes or with ^{177}Lu for therapy following the theranostics paradigm [17]. ^{177}Lu-Somatostatin has been the first of the two to be used starting in the early 1990s. Lessons learned from the studies on treatment of metastatic NETs were that bone marrow suppression, and even myelodysplastic syndrome may be a side effect in patients treated with high dosages of >100 GBq (>3 Gy bone marrow radiation dose), therefore radiation dosimetry after each therapy is essential for individual optimization of future doses [18, 19]. However it should be noted that bone marrow involvement by itself is effectively controlled by PRRT, with long progression-free survival and overall survival [20].

Clinical data on the role of ^{177}Lu-PSMA for treatment of patients with metastatic prostate cancer is being accumulated. It appears that this mode of therapy is effective and safe in patients that are appropriately selected [21]. Diffuse bone marrow involvement is a risk factor for significant myelosuppression but could be identified by ^{68}GA PSMA imaging in advance [22]. It has been shown that as high as 58% with bone metastases treated with ^{177}Lu-PSMA report reduction in bone pain [23].

The forth PET tracer that can be used for assessment of skeletal bone involvement is ^{18}F-Fluoride. In contrast with the three earlier discussed tracers that accumulate directly in the tumor tissue, ^{18}F-Fluoride is a PET bone-seeking agent with uptake mechanism similar to that of ^{99m}Tc-MDP. Fluoride ions exchange with hydroxyl groups in hydroxyapetite crystal bone to form fluoroapatite, and are deposited at the bone surface where bone turnover is greatest. Similarly to ^{99m}Tc-MDP, accumulation of ^{18}F-Fluoride uptake in bone metastases reflects increased regional blood flow and high bone turnover, secondary changes occurring in bone as reaction to the presence of tumor cells. ^{18}F-Fluoride has better pharmacokinetic characteristics compared to those of ^{99m}Tc-MDP. The bone uptake of the former is two-fold higher, in contrast with ^{99m}Tc-MDP it does not bind to protein. The capillary permeability of ^{18}F-Fluoride is higher and its blood clearance is faster resulting in a better target- to-background ratio. Regional plasma clearance of ^{18}F-Fluoride was reported to be 3–10 times higher in bone metastases compared with that in normal bone [7, 24].

^{18}F-Fluoride-PET is very sensitive for detection of not only osteoblastic metastases but also of lytic ones, as the latter even when considered “pure lytic”, do have minimal osteoblastic activity which is enough for detection by ^{18}F-Fluoride-PET. It should be borne in mind that ^{18}F-Fluoride is not tumor specific and therefore is a sensitive modality for detection of any bone abnormalities, not only malignant.

When interpreting ^{18}F-Fluoride-PET-CT for assessment of metastatic skeletal spread, the morphologic appearance of the bone should be carefully considered on the CT data for accurate separation of benign and malignant sites of ^{18}F-Fluoride uptake [25–28].

References

1. Cook GJ, Fogelman I (2001) The role of positron emission tomography in skeletal disease. Semin Nucl Med 31:50–61
2. Even-Sapir E (2005) Imaging of malignant bone involvement by morphologic, scintigraphic, and hybrid modalities. J Nucl Med 46:1356–1367
3. Taira AV, Herfkens RJ, Gambhir SS et al (2007) Detection of bone metastases: assessment of integrated FDG PET/CT imaging. Radiology 243:204–211
4. Metser U, Lerman H, Blank A et al (2004) Malignant involvement of the spine: assessment by ^{18}FFDG PET/CT. J Nucl Med 45:279–284
5. Taïeb D, Hicks RJ, Pacak K (2016) Nuclear medicine in cancer theranostics: beyond the target. J Nucl Med 57(11):1659–1660
6. Hamaoka T, Madewell JE, Podoloff DA et al (2004) Bone imaging in metastatic breast cancer. J Clin Oncol 22:2942–2953
7. Grant FD, Fahey FH, Packard AB et al (2008) Skeletal PET with ^{18}F-fluoride: applying new technology to an old tracer. J Nucl Med 49:68–78
8. Cook GJR, Houston S, Rubens R et al (1998) Detection of bone metastases in breast cancer by ^{18}FDG PET: differing metabolic activity in osteoblastic and osteolytic lesions. J Clin Oncol 16(10):3375–3379
9. Maecke HR, Hofmann M, Haberkorn U (2005) 68 Ga-labeled peptides in tumor imaging. J Nucl Med 46(1):172S–175S
10. Putzer D, Gabriel M, Henninger B et al (2009) Bone metastases in patients with neuroendocrine tumor: ^{68}Ga-DOTA-Tyr3-octreotide PET in comparison to CT and bone scintigraphy. J Nucl Med 50(8):1214–1221
11. Gabriel M, Decristoforo C, Kendler D et al (2007) ^{68}Ga-DOTA-Tyr3-octreotide PET in neuroendocrine tumors: comparison with somatostatin receptor scintigraphy and CT. J Nucl Med 48: 508–518
12. Rauscher I, Maurer T, Fendler WP et al (2016) ^{68}Ga-PSMA ligand PET/CT in patients with prostate cancer: how we review and report. Cancer Imaging 16(1):14
13. Pyka T, Okamoto S, Dahlbender M et al (2016) Comparison of bone scintigraphy and ^{68}Ga-PSMA PET for skeletal staging in prostate cancer. Eur J Nucl Med Mol Imaging 43(12):2114–2121
14. Maurer T, Gschwend JE, Rauscher I et al (2016) Diagnostic efficacy of gallium-PSMA positron emission tomography compared to

conventional imaging in lymph node staging of 130 consecutive patients with intermediate to high risk prostate cancer. J Urol 195(5):1436–1443
15. Du Y, Cullum I, Illidge TM et al (2007) Fusion of metabolic function and morphology: sequential [18F]fluorodeoxyglucose positron-emission tomography/computed tomography studies yield new insights into the natural history of bone metastases in breast cancer. J Clin Oncol 25(23):3440–3447
16. Katayama T, Kubota K, Machida Y et al (2012) Evaluation of sequential FDG-PET/CT for monitoring bone metastasis of breast cancer during therapy: correlation between morphological and metabolic changes with tumor markers. Ann Nucl Med 26:426–435
17. Weineisen M, Schottelius M, Simecek J et al (2015) ^{68}Ga- and 177Lu-labeled PSMA I&T: optimization of a PSMA-targeted theranostic concept and first proof-of-concept human studies. J Nucl Med 56(8):1169–1176
18. Forrer F, Krenning EP, Kooij PP et al (2009) Bone marrow dosimetry in peptide receptor radionuclide therapy with [177Lu-DOTA(0),Tyr(3)] octreotate. Eur J Nucl Med Mol Imaging 36(7):1138–1146
19. Kam BL, Teunissen JJ, Krenning EP et al (2012) Lutetium-labelled peptides for therapy of neuroendocrine tumours. Eur J Nucl Med Mol Imaging 39(Suppl 1):S103–S112
20. Ezziddin S, Sabet A, Heinemann F et al (2011) Response and long-term control of bone metastases after peptide receptor radionuclide therapy with 177Lu-octreotate. J Nucl Med 52:1197–1203
21. Baum RP, Kulkarni HR, Schuchardt C et al (2016) 177Lu-labeled prostate-specific membrane antigen Radioligand therapy of metastatic castration-resistant prostate cancer: safety and efficacy. J Nucl Med 57(7):1006–1013
22. Heck MM, Retz M, D'Alessandria C et al (2016) Systemic Radioligand therapy with (177)Lu labeled prostate specific membrane antigen ligand for imaging and therapy in patients with metastatic castration resistant prostate cancer. J Urol 196(2):382–391
23. Kratochwil C, Giesel FL, Stefanova M et al (2016) PSMA-targeted radionuclide therapy of metastatic castration-resistant prostate cancer with 177Lu-labeled PSMA-617. J Nucl Med 57(8):1170–1176
24. Blake GM, Park-Holohan SJ, Cook GJR et al (2001) Quantitative studies of bone with the use of ^{18}F-fluoride and 99mTc-methylene diphosphonate. Semin Nucl Med 31:28–49
25. Even-Sapir E, Metser U, Flusser G et al (2004) Assessment of malignant skeletal disease: initial experience with ^{18}F-fluoride PET/CT and comparison between ^{18}F-fluoride PET and ^{18}F-fluoride PET/CT. J Nucl Med 45:272–278
26. Even-Sapir E, Metser U, Mishani E et al (2006) The detection of bone metastases in patients with high risk prostate cancer: 99mTc MDP planar bone scintigraphy, single and multi field of view SPECT, ^{18}F-fluoride PET and ^{18}F-fluoride PET/CT. J Nucl Med 47:287–297
27. Bortot DC, Amorim BJ, Oki GC, Gapski SB et al (2012) ^{18}F-fluoride PET/CT is highly effective for excluding bone metastases even in patients with equivocal bone scintigraphy. Eur J Nucl Med Mol Imaging 39:1730–1736
28. Even-Sapir E (2014) ^{18}F-fluoride PET/computed tomography imaging. PET Clin 9(3):277–285
29. Cook GJR (2010) PET and PET/CT imaging of skeletal metastases. Cancer Imaging 10:153–160